JOURNAL OF AIRCRAFT
Vol. 45, No. 1, January–February 2008

General Approach to Enhance Flying Qualities via Dynamic Balancing of Aircraft Mass

S. M. Malaek* and A. Karimi†
Sharif University of Technology,
11365-8639 Tehran, Iran

DOI: 10.2514/1.29372

This work describes a new mathematical model to predict the so-called aircraft handling qualities via proper positioning of aircraft mass in the early stages of the design process. The methodology aims to help make handling qualities and therefore pilot rating an integral part of the design process. The main idea is to find proper mass distributions for an aircraft in given flight conditions based on the well-known quantitative measures of flying qualities described in military standards. The proposed methodology allows aircraft designers to associate a density to different segments of an aircraft and have a prior insight about an optimum arrangement of internal parts such as fuel tanks, payload containers, passenger seats, and other massy items. Moreover, a new global optimization algorithm based on the Nelder–Mead Simplex method is devised to effectively solve the resulting optimization problem. This work shows how a B-747-100 could be mass balanced to achieve level-I flying qualities for both cruising and turning flights without using any stability augmentation system. Furthermore, the idea of a minimum effort generic control system is introduced that helps reduce the cost of aircraft certification.

Nomenclature

A	=	aircraft system matrix
B	=	control matrix
b	=	span
C	=	aerodynamic or control derivatives
$\bar{c}$	=	mean aerodynamic chord
f_A	=	force components due to aerodynamic
f_T	=	force components due to thrust
g	=	gravity constant
$I_{xx}, I_{yy}, I_{zz}, I_{xz}$	=	moments of inertia in body axes
m	=	total aircraft mass
P_1, Q_1, R_1	=	steady-state rotational velocity components
p, q, r	=	perturbation components of rotational velocity
S	=	wing area
U_1, V_1, W_1	=	steady-state velocity components
u, v, w	=	perturbed components of velocity
$\bar{u}$	=	control vector
X	=	aircraft state vector
$X_{\text{c.g.}}$	=	longitudinal position of center of gravity
α	=	angle of attack
β	=	sideslip angle
$\delta_E, \delta_A, \delta_R$	=	deflections of elevator, ailerons, and rudder
ζ	=	damping ratio of mode shape
Ψ_1, Θ_1, Φ_1	=	steady-state Euler angles
ψ, θ, φ	=	perturbation components of Euler angles
ω_n	=	natural frequency of mode shape

I. Introduction

THE idea of mass distribution management (MDM) to enhance aircraft dynamic characteristics and handling qualities was first proposed in [1]. However, the MDM methodology, although sound in its nature, leads to an optimization problem with complex mathematical form that is very difficult to solve. Malaek and Soltan-Mohammed in [1], in fact, fall short of offering any rigorous mathematical form to solve the resulting set of equations and leave it to some trial and error scheme to find some alternatives for aircraft mass distribution that satisfy the constraints. However, this work describes a mathematically sound and rigorous algorithm for the MDM and its relation with airplane flying qualities (FQ) [2]. The term "flying qualities" defines those characteristics and qualities of an aircraft, which govern the ease and precision with which a pilot is able to perform the tasks required in support of an aircraft role [2]. Obviously, the very existence of the pilot as an active control element (operator) justifies the study of FQ. While dealing with a new aircraft or new missions, the best way is still to collect actual pilot opinion. The current practice, however, to collect pilot opinion is to ask him about the relevance of the task he is supposed to do with the capabilities provided to him by the aircraft. Obviously, a design team would not have access to pilot's comments unless a prototype is built and flown [3], which would be very costly indeed, as we normally need more than one prototype. An alternative to this would be the use of a so-called "virtual prototyping" concept. This concept has been effectively used in the process of design and certification of A-380. Nevertheless, it requires a great deal of investment in computing power together with a precise physical model of the aircraft, which is still costly for smaller aircraft. In comparison, MDM once programmed is an efficient preliminary design tool and is less costly to use even for very large aircraft. Moreover, the results provided by the MDM technique give much better insight to the designer as to where to look for proper positioning of massy items.

Certifying a flight control system is still a costly process that repeats for any new aircraft. To ease the time and cost of the certification process, one might think of a generic flight control system, hereafter called the minimum effort generic control system (MEGCS). In the new approach, instead of developing a specialized control system for any new aircraft, one could concentrate on a class of aircraft with different takeoff weights. For example, one might think of developing a MEGCS for jet transports with takeoff weights between 4 to 800,000 pounds. In this approach, the design team focuses on reaching a dynamically well-behaved aircraft such that a MEGCS is sufficient to fly the aircraft safely. In this paper, authors present a methodology that leads to designing a dynamically well-behaved aircraft for a given class of weight and maneuverability. The description of the proposed MEGCS architecture needs more

Received 19 December 2006; revision received 8 May 2007; accepted for publication 15 May 2007.

*Professor, Aerospace Engineering Department, Post Office Box 11365-8639.

†Research Assistant, Aerospace Engineering Department, Post Office Box 11365-8639.

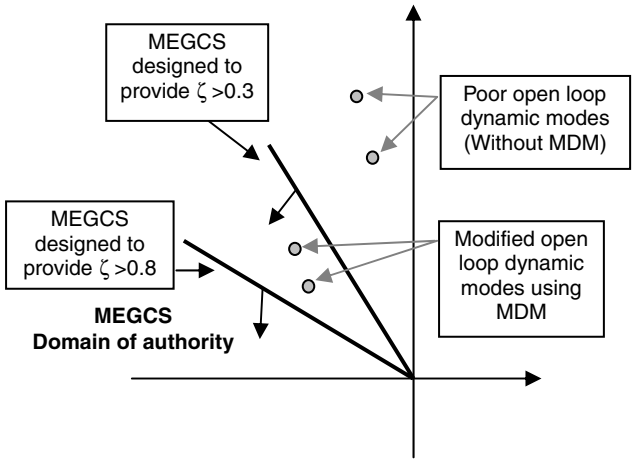

Fig. 1 General concept of MEGCS and the role of MDM.

elaboration and is beyond the scope of this paper [4]. In brief, because the desired positions for dynamic modes of all aircraft in one specific class are comparable [2], one could think of MEGCS as a means capable of driving the existing dynamic modes from their current position, wherever they are, to the desired ones in the S plane as suggested by applicable military standards (MIL) specifications. However, MEGCS, being a generic device, requires the existing dynamic modes to be literally "not too far" from the desired position that is a dynamically well-balanced aircraft. This is where the MDM technique plays its role, which is, paving the road to make a dynamically well-balanced aircraft. Figure 1 schematically shows the idea of MEGCS and the importance of the MDM technique. As seen, one might think of different MEGCS with different capabilities; each could be capable of dealing with dynamic modes within a certain distance from a desired position regardless of the aircraft external shape. Therefore, one might think of MDM not only as a mathematical design tool but also as a new approach in design of flying vehicles that considerably increases designers control over aircraft configuration.

II. MDM and Design Process

From an engineering point of view, it is very helpful to describe the flying qualities of an aircraft in terms of quantitative measures such as frequencies and damping ratios resulting from mathematical models of aircraft dynamics [3]. However, besides the so-called mass distribution management technique proposed in [1], no other systematic methodology has been presented in the literature. The need to involve FQ in the early stages of the design process where the design team has still considerable freedom in configuring the aircraft provides great flexibility and therefore is quite desirable. However, as described in [1], the MDM technique would not normally lead to a straightforward mathematical form and we still need to convert it to a suitable design tool for a preliminary design process. This paper presents a rigorous mathematical algorithm to support use of the MDM technique in such stages. A transparent correlation between quantitative measures of HQ and aircraft mass distribution forms the basis of the new algorithm. The proposed method, although applicable for different types of aircraft, is more useful for aircraft that accept different missions and payload arrangements. For such types as heavy transports, applying the MDM technique for different flight conditions allows the designer to place massy items like fuel tanks and baggage in a more efficient manner and thus designing a dynamically well-balanced aircraft. The next section describes aircraft general equations of motion, which form the basis of mathematical formulation.

A. Aircraft Equations of Motion

Roskam [3] provides an elaborate method to develop aircraft equations of motion, summarized by Eqs. (1) and (2):

$$\begin{cases} m(\dot{u} - V_1 r - R_1 v + W_1 q + Q_1 w) = -mg\theta\cos(\Theta_1) + f_{A_X} + f_{T_X} \\ m(\dot{v} + U_1 r + R_1 u - W_1 p - P_1 w) = -mg\theta\sin(\Phi_1)\sin(\Theta_1) + mg\phi\sin(\Phi_1)\sin(\Theta_1) + f_{A_Y} + f_{T_Y} \\ m(\dot{w} - U_1 q - Q_1 u + V_1 p + P_1 v) = -mg\theta\cos(\Phi_1)\sin(\Theta_1) - mg\phi\sin(\Phi_1)\cos(\Theta_1) + f_{A_Z} + f_{T_Z} \\ I_{xx}\dot{p} - I_{xz}\dot{r} - I_{xz}(P_1 q + Q_1 p) + (I_{zz} - I_{yy})(R_1 q + Q_1 r) = l_A + l_T \\ I_{yy}\dot{q} + (I_{xx} - I_{zz})(P_1 r + R_1 p) + I_{xz}(2P_1 p - 2R_1 r) = m_A + m_T \\ I_{zz}\dot{r} - I_{xz}\dot{p} + (I_{yy} - I_{xx})(P_1 q + Q_1 p) + I_{xz}(Q_1 r + R_1 q) = n_A + n_T \end{cases} \tag{1}$$

$$\begin{cases} p = \dot{\phi} - \dot{\Psi}_1\theta\cos(\Theta_1) - \dot{\psi}\sin(\Theta_1) \\ q = -\dot{\Theta}_1\phi\sin(\Phi_1) + \dot{\theta}\cos(\Phi_1) + \dot{\Psi}_1\phi\cos(\Theta_1)\cos(\Phi_1) - \dot{\Psi}_1\theta\sin(\Theta_1)\sin(\Phi_1) + \dot{\psi}\cos(\Theta_1)\sin(\Phi_1) \\ r = -\dot{\Psi}_1\phi\cos(\Theta_1)\sin(\Phi_1) - \dot{\Psi}_1\theta\sin(\Theta_1)\cos(\Phi_1) + \dot{\psi}\cos(\Theta_1)\cos(\Phi_1) - \dot{\Theta}_1\phi\cos(\Phi_1) - \dot{\theta}\sin(\Phi_1) \end{cases} \tag{2}$$

Equation (1) is a set of six linear-coupled equations in terms of nine motion variables: u, v, w, p, q, and r and three Euler angles ψ, θ, and φ. The set of equations in Eq. (2) are so-called "kinematic equations" and are used to solve for derivatives of motion variables [3]. Solving Eqs. (1) and (2) for time derivatives of motion variables leads to the state-space representation of aircraft dynamics, given by Eq. (3), where A and B are the system and control matrices, respectively,

$$\dot{\boldsymbol{X}} = A\boldsymbol{X} + B\boldsymbol{u} \tag{3}$$

While dealing with the subject of aircraft flying qualities, it proves to be easier to work with the so-called "dynamic mode shapes" rather than time responses of the aircraft. Mode shapes are related to roots of the aircraft dynamic characteristics equation (DCE), given by ($|A| = 0$). For a known flight condition together with external shape, total weight, and mass distribution properties, one could calculate elements of matrix [A] in a straightforward manner. The roots of the aircraft DCE are known as open loop dynamic modes. For a rigid conventional aircraft, there are normally nine roots that form the dynamic modes in each flight condition. These are short-period, phugoid, Dutch-roll, spiral, and roll modes. Because of the neutral stability of any aircraft in the heading angle, one of the roots is always at the origin [3].

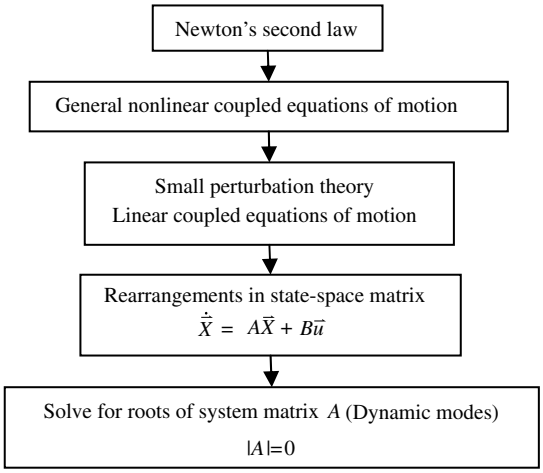

Fig. 2 General procedure to derive equations of motion and dynamic modes.

With DCE resulting from $|A| = 0.0$, one could easily describe aircraft dynamic characteristics in the S domain [3]. A linear-coupled state-space representation of the aircraft dynamics, such as Eq. (3), consisting of both longitudinal and lateral–directional equations is sufficient for a preliminary design purpose [3] and application of MDM. Figure 2 shows the general procedure to extract the appropriate state-space equations as well as dynamic modes as used for the MDM technique.

Considering Fig. 2, to obtain the elements of $[A]$ in a given flight condition, one needs to solve the associated trim equations for all desired maneuvers. Here, we consider a "coordinated level turn" as a maneuver in which the coupling effects are more likely to occur. Equation (4) gives the trim equations with five unknowns of angle of attack (α_1) and sideslip angle (β_1) along with three control surface deflections (δ_E, δ_R, and δ_A). Both α_1 and β_1 appear directly in the system dynamic matrix $[A]$. Knowing that the set of equations given by Eq. (1) is in the stability axes, one could use α_1 to transform values of mass moments of inertia from the body axes to the stability axes [3]. It is worth noting that a level turn is normally characterized by a steady-state bank angle, Θ_1. Therefore, cruising flight might also be investigated by setting Φ_1 to zero; that is, Eq. (4) is applicable for both cruise and turning flight conditions:

$$\begin{cases} Z_1 = 0 = C_{L_0} + C_{L_\alpha}\alpha + C_{L_q}\frac{Q_1\bar{c}}{2U_1} + C_{L_{\delta E}}\delta E - \frac{mg}{\bar{q}S\cos(\Phi_1)} \\ M_1 = 0 = C_{m_0} + C_{m_\alpha}\alpha + C_{m_q}\frac{Q_1\bar{c}}{2U_1} + C_{m_{\delta E}}\delta E + \frac{I_{xzS}R_1^2}{\bar{q}S\bar{c}} \\ Y_1 = 0 = C_{Y_\beta}\beta + C_{Y_r}\frac{R_1 b}{2U_1} + C_{Y_{\delta A}}\delta A + C_{Y_{\delta R}}\delta R \\ L_1 = 0 = C_{l_\beta}\beta + C_{l_r}\frac{R_1 b}{2U_1} + C_{l_{\delta A}}\delta A + C_{l_{\delta R}}\delta R - \frac{(I_{zzS}-I_{yyS})R_1 Q_1}{\bar{q}Sb} \\ N_1 = 0 = C_{n_\beta}\beta + C_{n_r}\frac{R_1 b}{2U_1} + C_{n_{\delta A}}\delta A + C_{n_{\delta R}}\delta R - \frac{I_{xzS}R_1 Q_1}{\bar{q}Sb} \end{cases} \tag{4}$$

B. Basics of Handling Quality and MIL-8785-C

Any new type of aircraft designed for new missions demands research on the appropriate handling qualities in a systematic manner [5,6]. In this work, to determine how well an aircraft is dynamically balanced, we use MIL-8785-C as an acceptable criterion [2]. This standard describes flying quality requirements in terms of upper and lower limits for damping and frequencies of a class of aircraft (I, II, III, and VI), in a given flight phase (A, B, C). In other words, the requirements normally limit natural frequencies, damping ratios, and/or time constants and characteristics of the time responses. For each class of aircraft appropriate limits for dynamic modes to satisfy a level-I flying quality are specified, which are sufficient for the aircraft preliminary design [3].

Once the damping and frequencies of each mode are determined, one might check them against requirements such as those proposed in [2]. This leads to identifying whether the aircraft would have level-I, level-II, or level-III flying qualities. Table 1 repeats the necessary requirements to have level-I flying qualities for a typical heavy transport (class III) in cruising flight [phase (B)]. These requirements are treated as constraints while we solve for the optimized mass distribution of the aircraft. In this work, we require level-I flying qualities in selected maneuvers based on MIL-8785-C.

C. MDM Role in Preliminary Design

A differentiable change to the mass distribution of an aircraft would obviously result in changes in its mass moments of inertias around all axes ($I_{xx}, I_{yy}, I_{zz}, I_{xz}$) together with changes in the center of gravity (c.g.) position and therefore the static margin (SM). These parameters play important roles in the dynamic behavior of the aircraft [6]. The overall role of MDM is therefore to keep all moments of inertia as well as the c.g. position within certain limits dictated by dynamic mode shapes throughout the stages of design [1]. To further clarify the mathematical approach, one might consider equations given by Eq. (5) which represent the relationship between aircraft mass distribution and static margin as well as some important stability derivatives. The superscript zero indicates the current or nominal values of the parameters:

$$\begin{cases} C_{m_\alpha} = -C_{L_\alpha}\cdot \mathrm{SM} \\ C_{m_0} = C^0_{m_0} - C_{L_0}\cdot(\mathrm{SM} - \mathrm{SM}^0) \\ C_{m_q} = C^0_{m_q} - C_{L_q}\cdot(\mathrm{SM} - \mathrm{SM}^0) \\ C_{n_r} = C^0_{n_r} - C_{Y_r}\cdot(\mathrm{SM} - \mathrm{SM}^0) \\ C_{n_\beta} = C^0_{n_\beta} - C_{Y_\beta}\cdot(\mathrm{SM} - \mathrm{SM}^0) \end{cases} \tag{5}$$

Based on Eq. (5), one might relate aircraft mass distribution to its dynamic behavior (FQ) through inertia terms of $I_{xx}, I_{yy}, I_{zz}, I_{xz}$, and $X_{\mathrm{c.g.}}$. With this, the process of MDM could be divided into two phases. In the first phase, we search for an optimum set of inertia properties that provides the most desirable static as well as dynamic stability prescribed by MIL specifications. This phase is named the "inertia management" phase, which leads to some upper and lower bounds for aircraft inertia properties. One needs to repeat this calculation for all applicable flight conditions based on the aircraft mission. The outcomes of this phase are some sets of inertia properties that are either selected for implementation based on experience or other suitability measures such as similarity with previous designs. Obviously, this process could well become complicated as the number of flight conditions increases. In that case, a computer program might be used to compare the results based on some selection criterion that selects the most appropriate set of inertia properties. Figure 3 summarizes this procedure.

The last step in Fig. 3 may vary according to the way one desires to define optimality in the overall MDM process. That is, one might use the algorithm to optimize inertia properties in a certain flight

Table 1 Level-I requirements for class III in flight phase B

Mode shape	Roll	Spiral	Dutch roll	Phugoid	Short period
FQ requirements	$\tau < 1.4$ s	$t_{2A} > 20$ s	$\zeta > 0.08$ $\omega_n > 0.4$ $\zeta\cdot\omega_n > 0.15$	$\zeta > 0.04$	$0.3 < \zeta < 2.0$ $0.98 < \omega_n < 6.54$

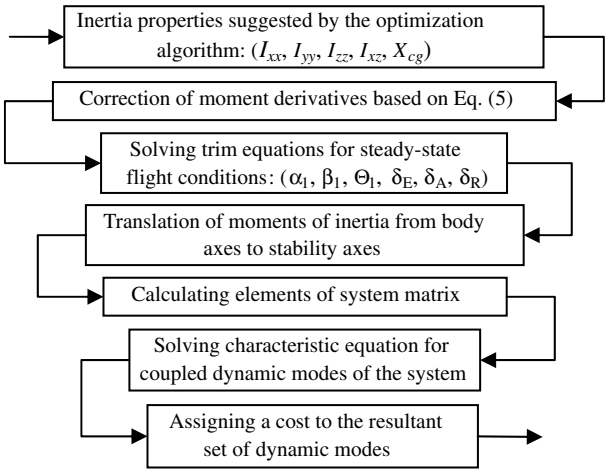

Fig. 3 General algorithm to select a set of inertia properties within the optimization algorithm.

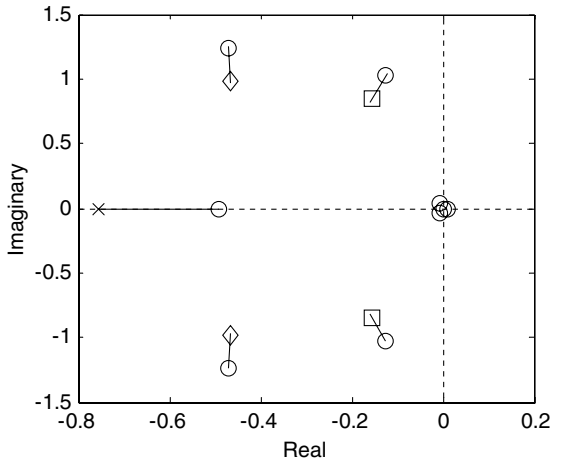

Fig. 4 Example of cost function evaluation in mass property optimization [desired values of roll (×), Dutch roll (□), and short-period (◇) versus their current positions (○)].

condition such that the open loop dynamic modes get as close to some predefined positions as possible. In other approaches, all applicable sets of inertia properties for all required flight conditions are calculated and the one that receives the highest overall grade is selected as the candidate solution. Regardless of which approach one might use, the key point is to bring the open loop modes into some desired predefined positions via optimization of mass properties. Once this task is completed, the rest is left to the design team to modify the resulting optimal set based on other requirements such as inspection and maintenance.

Figure 4 shows a typical set of open loop modes together with their desired positions. Normally, there are five inertia properties (I_{xx}, I_{yy}, I_{zz}, I_{xz}, $X_{c.g.}$), and so we are able to adjust up to a maximum of five unknowns in the mathematical structure of the open loop dynamic modes. This could be either two oscillatory modes and one nonoscillatory time constant or one oscillatory mode and three nonoscillatory time constants. Nevertheless, this might not seem attractive at first glance. However, noting that regions and not exact boundaries define flying quality requirements, one could take advantage of this to move more than five mode characteristics to desirable regions. In this approach, the cost associated with a given arrangement of modes is calculated by adding distances between the desired locations and the current locations of modes.

Once a suitable set of inertia properties is selected, we proceed to find any possible mass distribution that delivers such properties. A typical mass distribution model of an aircraft is shown in Fig. 5. In this model, the whole aircraft is seen as a collection of nodes with appropriate density value assigned to each node. Between any two adjacent nodes, the mass properties including density and gyration radius are assumed to vary linearly. The density values at each node are unknowns that the optimization algorithm finds for a given total weight and inertia properties. This constraint, however, leads to an unnecessary long computation time. To avoid such complexities, one might scale all density values by a factor such as (M_{ac}/M_{sl}), where M_{ac} is the total mass of the aircraft, a known constant, and M_{sl} is the total mass proposed by the optimization algorithm. Using the scaled density values, one could determine the c.g. position for the complete aircraft. This might be done by taking the c.g. position and inertias of each segment, and translating them to the aircraft c.g. position. Obviously, for I_{xz}, one needs to calculate I_{xz} of all segments with respect to any arbitrary point, such as the aircraft c.g. position. Finally, the sum of the differences between calculated and desired values is returned as the weight factor associated with the solution at hand. This approach is more accurate than the lumped mass model of [1], because the contribution of each segment local moment of inertia (around its own axes) is taken into account.

Once the optimization algorithm converges to a set of optimal values for nodal densities, the second phase of MDM is completed. In most cases, there would be more than one candidate solution, so one needs to properly evaluate all resulting mass distributions. From a mathematics perception, a more refined model with more nodes would not necessarily provide better solutions, as it increases the number of optimal candidates. Obviously, some mass distributions might not be acceptable as far as state-of-the-art manufacturing technology is concerned. In such cases, relaxing the requirements and searching for a near-optimal solution increases the chance of finding a more acceptable mass distribution. The next section provides a discussion about how the optimization algorithms work.

III. Optimization Algorithms

To implement the MDM technique, one needs a continuous global optimization algorithm that aims at finding the global minimum of a continuous function f without being trapped into its local minima.

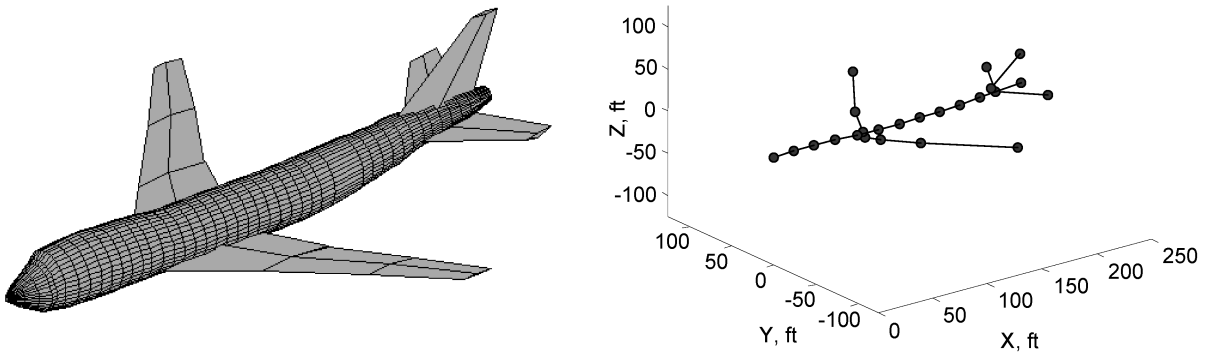

a) Actual aircraft **b) Mass distribution model**

Fig. 5 Mass distribution model based on actual aircraft shape.

Function f depends on a set of decision variables or design parameters $y := (y_1, y_2, \ldots, y_n)$ where each variable is limited by a lower and an upper bound. There are a number of mathematical algorithms in the literature that could deliver such capabilities. Among these techniques, one might see a special interest in evolutionary algorithms (EAs) and their various modifications. To solve the optimization problem resulting from MDM, we examined two recently introduced methods named the continuous genetic algorithm (CGA) and the continuous hybrid algorithm (CHA) [7,8]. CGA is a real-coded GA, which first locates the most promising areas of the search space and then continues the search through intensification inside those areas. CHA is a hybridization of CGA with the Nelder–Mead simplex search [9] that allows an intensification phase with more accuracy. Still, the poor performance of such methods in solving a typical MDM problem led to the development of a new global optimizer based on simplex search concepts. In the next sections, we describe how the new algorithm works.

A. Global Simplex Search (GSS)

The new algorithm devised to solve a typical MDM as an optimization problem is called the global simplex search (GSS), which is basically an EA using a randomized version of the reflection and expansion operations of the Nelder–Mead simplex search as its "recombination operator." The application of the simplex crossover (SPX) in genetic algorithms has already been investigated in several works [10–14]. However, only [15] deals with its integration to other branches of EA. Sotiropoulos et al. [15] present an EA, called the simplex evolution (SE) that replaces the "mutation operator" of the EA with a specially designed simplex operator. The simplex operator of SE has deterministic steps and consists of reflection, expansion, and contraction operations of the Nelder–Mead simplex search. By applying the designed simplex at each iteration of SE to any individual from the current generation, a new generation is obtained. This process continues until a stopping criterion is reached. The newly developed GSS, while exploiting the simplex scheme, has a different nature. Figure 6 shows the general flowchart of GSS. A brief description of different steps of GSS follows.

1. *Generation of the Initial Population*

A random initial population is generated in such a way that the minimum distance between the individuals is not larger than $d_{\min}$ of Eq. (6). One must observe the uniformity of the initial population to the extent possible as it has a considerable effect on the performance of the algorithm:

$$d_{\min} = \left(\frac{1}{N_{ip} \cdot \prod_{i=1}^{n} [L_u(i) - L_l(i)]} \right)^{1/n} \tag{6}$$

In Eq. (6), n is the problem dimension, $L_u(i)$ and $L_l(i)$ are the upper and lower limits of the ith design variable, and N_{ip} is the initial size of the population.

2. *Simplex Operators: Reflection and Expansion*

The iterations of GSS are executed in reflection or expansion modes based on the quality of the individuals created in the previous iteration. At the beginning of each iteration, if the search is in reflection mode, a new random simplex is constructed by random selection of $n + 1$ nonrepetitive individuals from the current population and then a reflection operation is applied. The reflection operation of Eq. (7) mirrors the worst vertex of the simplex s_{worst} with respect to the centroid of the other vertices $\bar{s}$; the result is a new individual s_r:

$$s_r = (1 + \alpha)\bar{s} - \alpha s_{\text{worst}} \tag{7}$$

In GSS, to give more freedom to the algorithm, the value of α is randomly selected from the interval $[\alpha_{\min}, \alpha_{\max}]$ according to a uniform probability distribution, where $\alpha_{\min}$ and $\alpha_{\max}$ are parameters of the algorithm. In this work, we set $[\alpha_{\min}, \alpha_{\max}] = [0.75, 1.25]$,

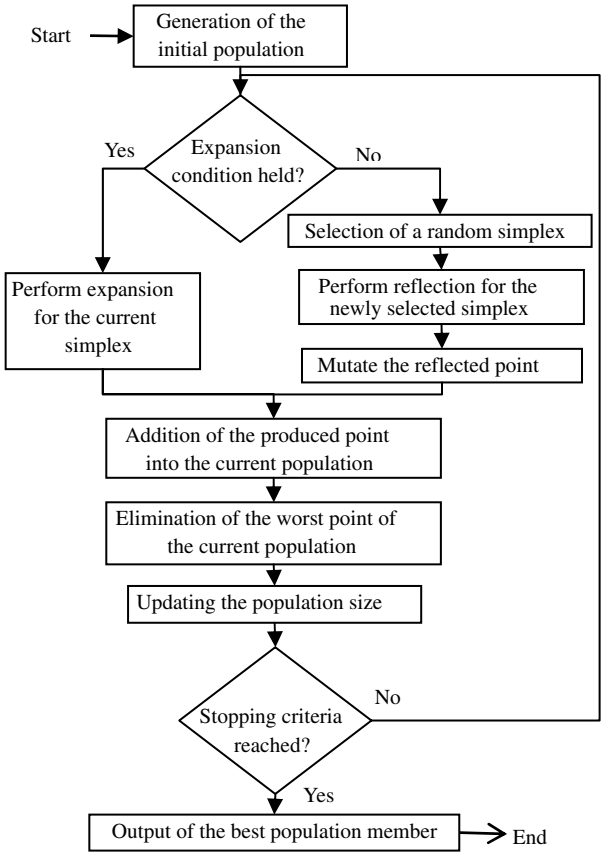

Fig. 6 General flowchart of GSS.

which proved to be a suitable setting for MDM problems. Once the reflection operation is completed, if $f(s_r)$ is better than all the simplex vertices, the search switches to the expansion mode. At the start of an iteration in the expansion mode, any individual s_{i-1} (generated in the previous iteration), is expanded in the direction of V_{ref} with a random step size given by Eq. (8), where V_{ref} is the vector connecting s_{worst} to $\bar{s}$:

$$s_e = s_{i-1} + N(1, \tfrac{1}{3})V_{\text{ref}} \tag{8}$$

In Eq. (8), $N(1, 1/3)$ is a Gaussian random number with mean of 1 and a standard deviation of $1/3$ and s_e is the result of the expansion operation.

3. *Mutation Operator*

In addition to simplex operators, GSS enjoys a mutation operator to increase its robustness. At this stage the results of both reflection

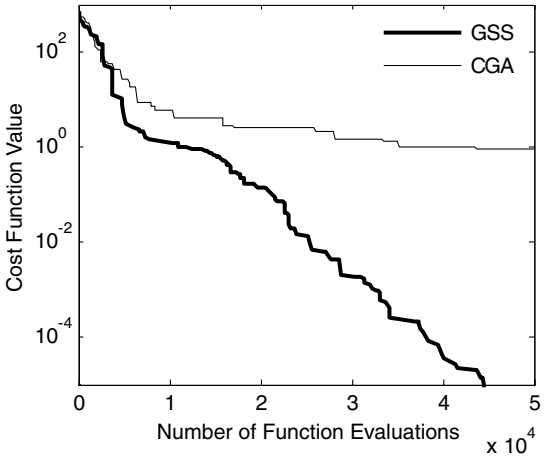

Fig. 7 Typical convergence rates of GSS and CGA.

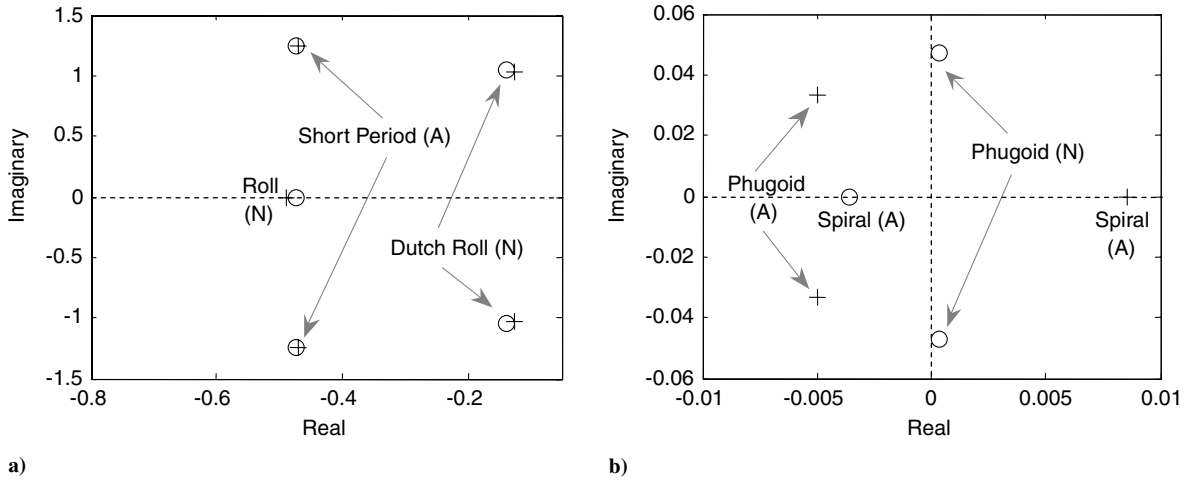

Fig. 8 B-747-100 open loop modes in high altitude cruise and level turn and their evaluation [acceptable (A) and not acceptable (N)].

and expansion go through a mutation process as follows. For each dimension of the problem, a uniformly random number is generated between 0 and 1 and if it is lower than the mutation rate, ρ_m, the ith component of the individual s is changed using Eq. (9):

$$s(i) = s(i) + N(0, \sigma) \tag{9}$$

In Eq. (9), $N(0, \sigma)$ is a random Gaussian number with mean of zero and standard deviation of σ. σ is the so-called "mutation strength," where in GSS, its value is fixed to $\max(i) - \min(i)/4$, where $\max(i)$ and $\min(i)$ are the upper and lower limits of the ith design variable. In MDM, the mutation rate is found to be the most appropriate while fixed to 0.05.

4. Updating the Population

In GSS, the population size gradually decreases as the search progresses. The change in the population size from its initial value N_{ip} to its final one N_{fp} could be logarithmically mapped into the decrease in error from its initial value in the initial population e_0 to its final value e_f, using Eq. (10), where e is the error value corresponding to the current iteration:

$$N_p = N_{ip} + [\log(e) - \log(e_0)]\frac{N_{fp} - N_{ip}}{\log(e_f) - \log(e_0)} \tag{10}$$

Using Eq. (10), if the closest integer value to N_p is larger than the current population size, the worst individual of the current population is eliminated. For MDM applications, the initial and final population sizes have been set to 100 and 50, respectively, and the final error to $1.0e-4$.

5. Stopping Criteria

The algorithm stops if the predefined acceptable accuracy of the solution, that is, e_f, a maximum number of objective function evaluations, or a maximum number of iterations is reached.

B. Global Simplex Search for MDM

Different case studies conducted to solve a MDM problem at a practical level proved CGA algorithms would not result any accurate answer [4], which satisfies the constraints. Figure 7 shows the convergence rates of GSS and CGA when applied to a typical MDM problem. In this specific example, CGA is run with different parameter settings such as "mutation probability" and "mutation type" and the best performance is selected for comparison. CGA normally leads to a premature convergence with a cost value less than 1.0. In comparison, GSS has a very good converging behavior and the accuracy of the solution will monotonically increase as the search continues. Karimi in [4] presents further discussion regarding performance of other search algorithms such as CHA.

IV. Case Studies

In this work, we use a B-747-100 as described in [3] to demonstrate how MDM and GSS could help modify the open loop dynamics of a typical transport. Figure 8 together with Table 2 shows

Table 2 Evaluation of B-747-100 based on [3]

		Cruise			Level turn		
Mode shape	Level-I requirements	Value	Properties	Evaluation	Value	Properties	Evaluation
Roll	$\tau < 1.4$ s	-0.490	$\tau = 2.041$ s	Unacceptable	-0.474	$\tau = 2.110$ s	Unacceptable
Spiral	$t_{2A} > 20$ s	0.008	$t_{2A} = 81$ s	Acceptable	-0.007	The mode is stable	Acceptable
Phugoid	$\zeta > 0.04$	$-0.005 \pm 0.033i$	$\omega_n = 0.034$, $\zeta = 0.148$	Acceptable	$0.002 \pm 0.041i$	$\omega_n = 0.041$, $\zeta = -0.058$	Unacceptable
Dutch roll	$\omega_n > 0.4$, $\zeta > 0.88$, $\zeta \cdot \omega_n > 0.15$	$-0.126 \pm 1.035i$	$\omega_n = 1.042$, $\zeta = 0.121$	Unacceptable	$-0.137 \pm 1.047i$	$\omega_n = 1.056$, $\zeta = 0.129$	Unacceptable
Short period	$0.3 < \zeta < 2.0$, $0.98 < \omega_n < 6.54$	$-0.471 \pm 1.237i$	$\omega_n = 1.324$, $\zeta = 0.356$	Acceptable	$-0.472 \pm 1.238i$	$\omega_n = 1.324$, $\zeta = 0.356$	Acceptable

Table 3 Current and optimized values of inertia properties (baseline design)

Inertia Properties	I_{xx}, slug · ft^2	I_{yy}, slug · ft^2	I_{zz}, slug · ft^2	I_{xz}, slug · ft^2	$X_{\text{c.g.}}$
Current value	18,200,000	33,100,000	49,700,000	970,000	100.536
Optimized value	11,284,000	33,100,000	42,742,000	970,000	103.510

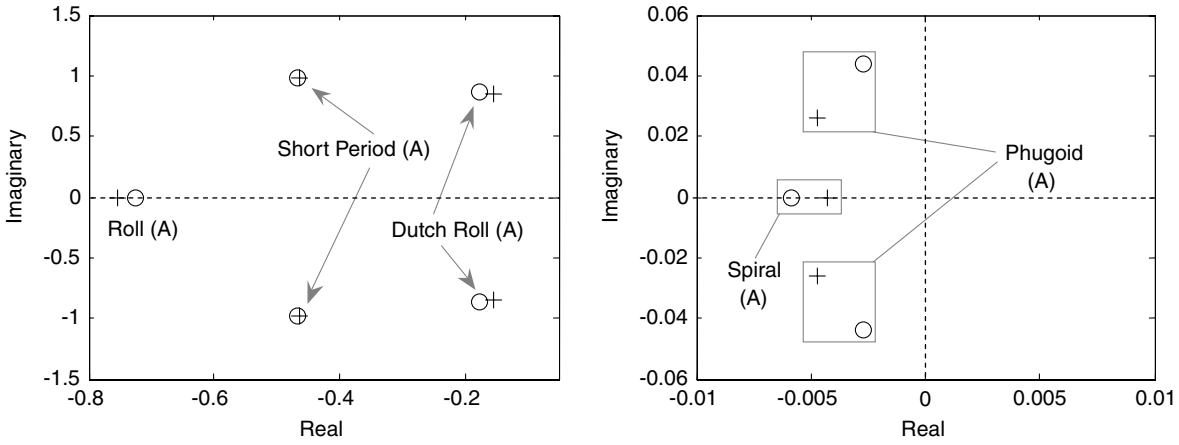

Fig. 9 Optimized open loop modes in high altitude/speed cruising and level turning flights and their evaluation [acceptable (A) and not acceptable (N)].

the existing conditions of the aircraft open loop dynamic modes for two different flight conditions, that is, high altitude cruise and level coordinated turn with a constant bank angle of 40 deg. Table 2 shows that the aircraft would not satisfy level-I requirements demanded by [2]. Therefore, we desire to enhance phugoid, roll, and Dutch-roll qualities of the aircraft to the level-I FQ by properly rearranging its mass distribution. The first step is to find a set of inertia properties which help bring poor dynamic modes in both flight conditions within level-I requirements. One could find a suitable set of inertia terms by running the first phase of the MDM technique (Table 3). Table 3 simply shows that B-747-100 needs some modification in its inertia terms to satisfy level-I requirements. We refer to the newly found inertia terms as the "baseline design" and knowing the fact that these values might not be practical, we try to tailor them to satisfy other available constraints in the second phase of the MDM technique. That is, we proceed to find an optimal mass distribution that could provide such moments of inertia. Figure 9 together with Table 4 shows the open loop dynamic modes of the aircraft with baseline properties. As seen, in both flight conditions, all modes, including phugoid, roll, and Dutch roll, are now satisfying level-I requirements.

We first investigate a mass model consisting of 14 nodes (Fig. 5). Figure 10 shows four possible solutions for this model, some of which are expected to be impractical. In the same figure, the Z axis represents the variations of mass density in slug/ft along the body and wing segments. In Fig. 5b, values of mass density at each section are given by the difference between the Z-axis values of the upper and lower points at each corresponding section. As one expects, some solutions might be unacceptable such as Fig. 10c and some might prove to be impractical, later on, during the implementation phase such as Fig. 10b. Solutions that exhibit excessively uneven distribution of mass in either fuselage or wing planform could readily be discarded. It is also interesting to note that other solutions given by the 14-node model (not shown here) are quite similar to the first distribution (Fig. 10a) with only slight differences in the fuselage mass distribution [4].

In the second trial, we examine a model consisting of 20 nodes. Figure 11 shows four possible distributions for this 20-node model. Solutions exhibit relatively better patterns and offer some choices for locating massy items for the aircraft at hand (local jumps in the mass distribution). For this aircraft, changing I_{xx} and I_{xz} has considerable effects on the resulting mass distribution patterns. Table 5 lists nine possible tailorings of the baseline design and Fig. 12 illustrates their associated mass distribution patterns. Figure 13 shows the plots of linear mass density along different segments of the aircraft for cases (b), (d), (f), and (i) from Fig. 12, which tend to be more practical.

Different case studies show that while tailoring a baseline design, there is always a region in which all FQ requirements are satisfied. This is true, at least for a good design such as B-747. However, it is usually desirable to evaluate the maximum allowable c.g. travel offered by various inertia properties. This is done by calculating the most fore and aft c.g. positions for each point in the design domain. Using such information, one could decide on the maximum allowable c.g. travel and the mean $X_{\text{c.g.}}$ associated with it. Figures 14–16 show the results of such calculations for three cases of cruising flight only, turning flight only, and their combination. A design space consisting of I_{xz} ranging from $-2.0\,e6$ to $+2.0\,e6$ slug $\cdot$ ft^2, I_{xx} ranging from $0.85\,e7$ to $1.15\,e7$ slug.ft^2, and the values of $X_{\text{c.g.}}$ between 95 and 105 ft have been examined. Considering the HQ in cruising flight only (Fig. 14), the lower limit for I_{xz} for a given I_{xx} is dictated by the quality of roll time constant and its upper limit is influenced by the behavior of the Dutch-roll mode. On the other hand, in turning flight (Fig. 15), no upper limit exists for I_{xz}. However, roll-mode time constant has a stronger influence on the lower limit of I_{xz} compared to that of the cruising flight. A similar conclusion could be made for the third case where both cruising as well as turning flight are under consideration.

Figures 14–16 are shaded to give a better presentation of the acceptable areas. One might note that the two shaded patterns in all figures are identical. This is due to the fact that the short-period mode dictates the most fore c.g. position while changing I_{xx} and I_{xz} has little or no effect on this mode, at least, in cruising flight. In turning flights, however, the most fore c.g. position slightly varies by changing I_{xx} and I_{xz}. This is due to coupling between the lateral and

Table 4 Evaluation of B-747-100 based on baseline mass properties

	Cruise			Level turn		
Mode shape	Value	Properties	Evaluation	Value	Properties	Evaluation
Roll	-0.754	$\tau = 1.326$ s	Acceptable	-0.725	$\tau = 1.380$ s	Acceptable
Spiral	-0.004	The mode is stable	Acceptable	-0.006	The mode is stable	Acceptable
Phugoid	$-0.005 \pm 0.026i$	$\omega_n = 0.026$, $\zeta = 0.181$	Acceptable	$-0.003 \pm 0.044i$	$\omega_n = 0.044$, $\zeta = 0.060$	Acceptable
Dutch roll	$-0.155 \pm 0.845i$	$\omega_n = 0.859$, $\zeta = 0.180$	Acceptable	$-0.176 \pm 0.864i$	$\omega_n = 0.881$, $\zeta = 0.200$	Acceptable
Short period	$-0.465 \pm 0.979i$	$\omega_n = 1.084$, $\zeta = 0.429$	Acceptable	$-0.465 \pm 0.980i$	$\omega_n = 1.084$, $\zeta = 0.429$	Acceptable

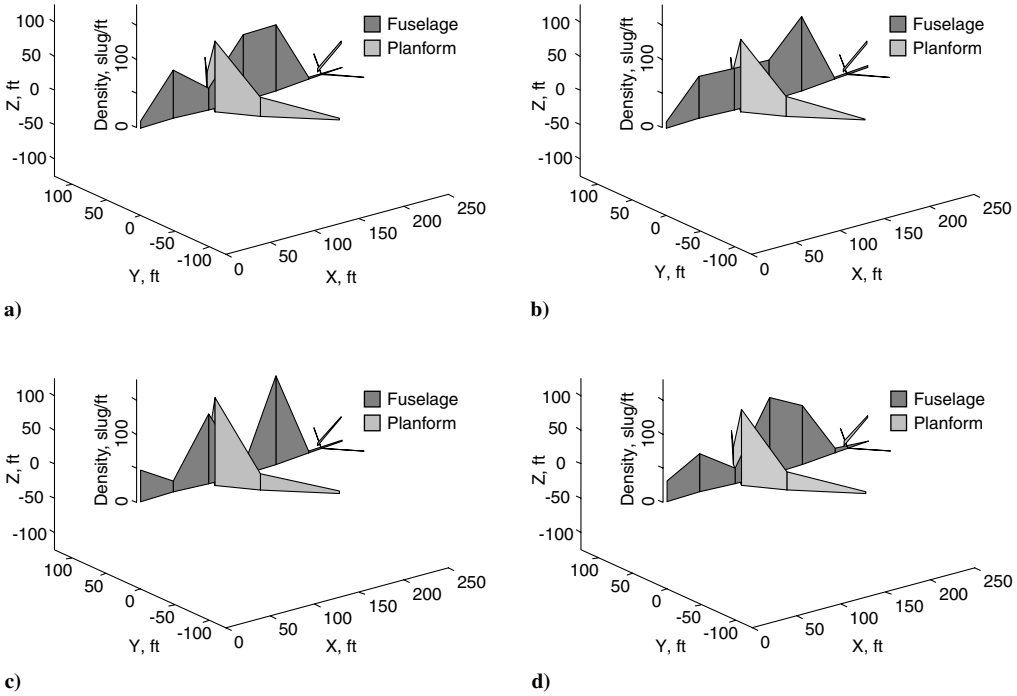

Fig. 10 Optimum mass distribution patterns for a 14-node mass model and baseline design.

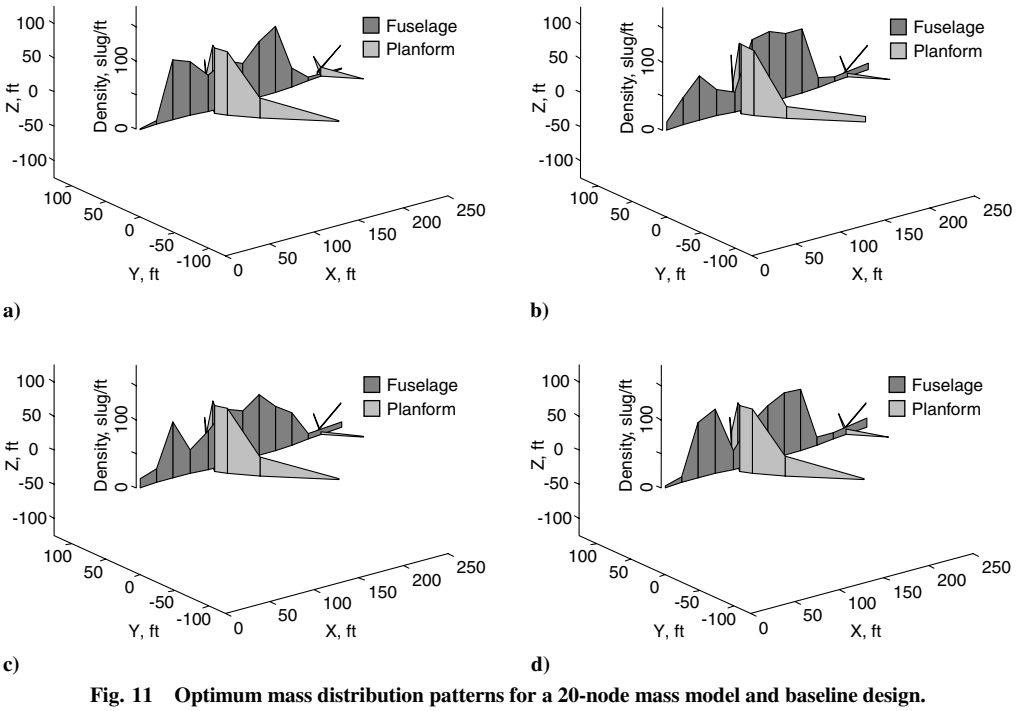

Fig. 11 Optimum mass distribution patterns for a 20-node mass model and baseline design.

Table 5 Tailoring the baseline design ($I_{xx} = 11,284,000$ slug · ft^2, $I_{xz} = 970,000$ slug · ft^2)

Corresponding distribution from Fig. 12	Change in I_{xx}, %	Change in I_{xz}, %
a	0	+13.40
b	−0.12	+23.71
c	−0.74	−12.37
d	−0.74	0
e	−0.74	+13.40
f	−0.74	+23.71
g	−2.52	−27.84
h	−2.52	−17.53
i	−2.52	+23.71

the longitudinal mode in this flight condition. In general, these changes are negligible compared to the large changes in the most aft c.g. position. However, despite the similar shading patterns in each pair, they represent different aspects of the c.g. traveling properties of the aircraft. In fact, considering the interval given by $[\min(X_{\text{c.g.}}) \max(X_{\text{c.g.}})]$, the right plot shows the movement of the interval, and the left one represents the way it expands and/or shrinks by selecting different inertia values.

Based on these observations, one could systematically examine each set of inertias in the feasible region. Obviously, regions insensitive to any c.g. travel (i.e., white shading) are more desirable. As seen, the designer still has plenty of freedom to consider other constraints and/or disciplines. However, as the figures suggest, this

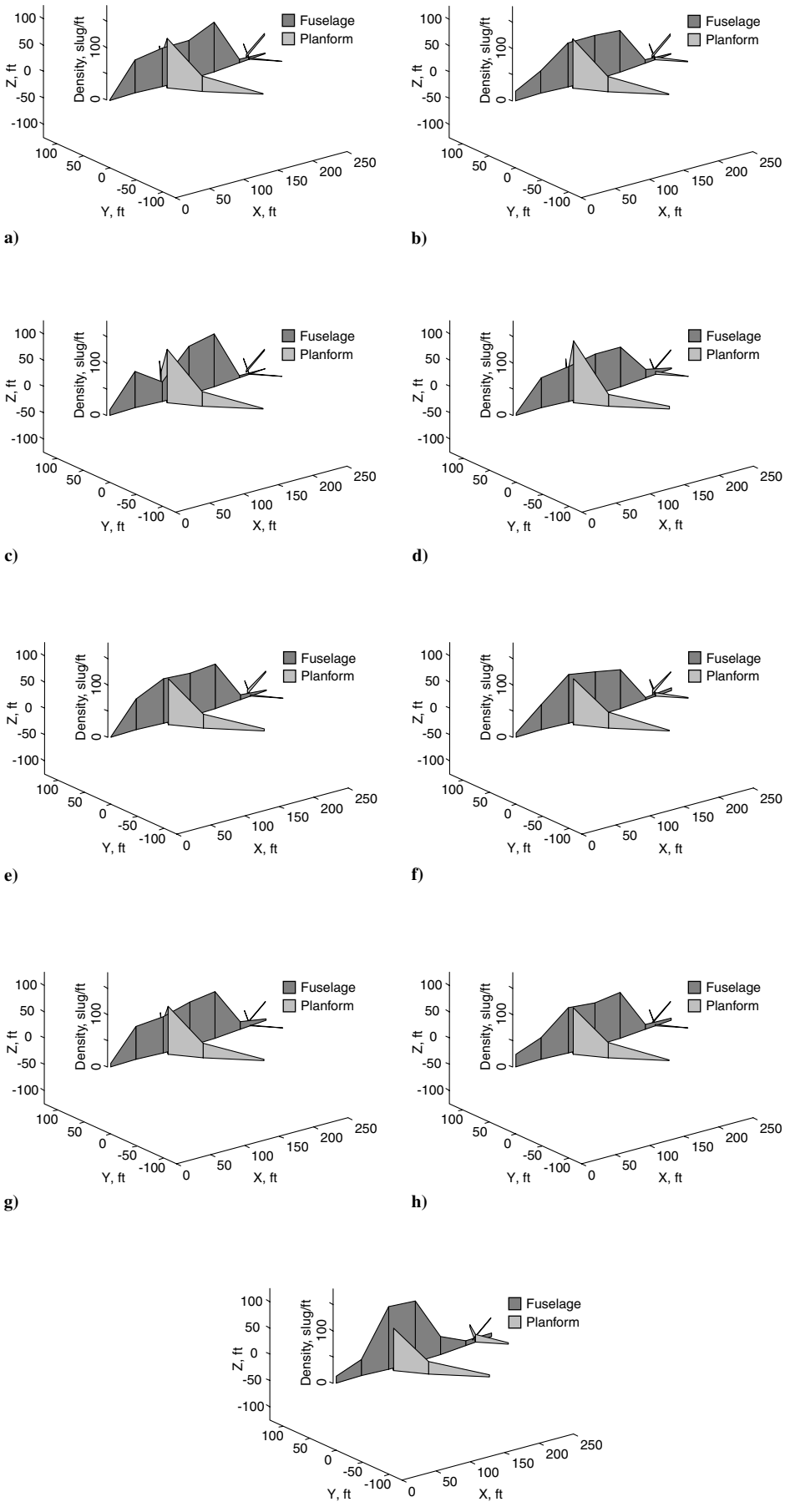

Fig. 12 Tailored optimum mass distribution patterns for 14-node mass model.

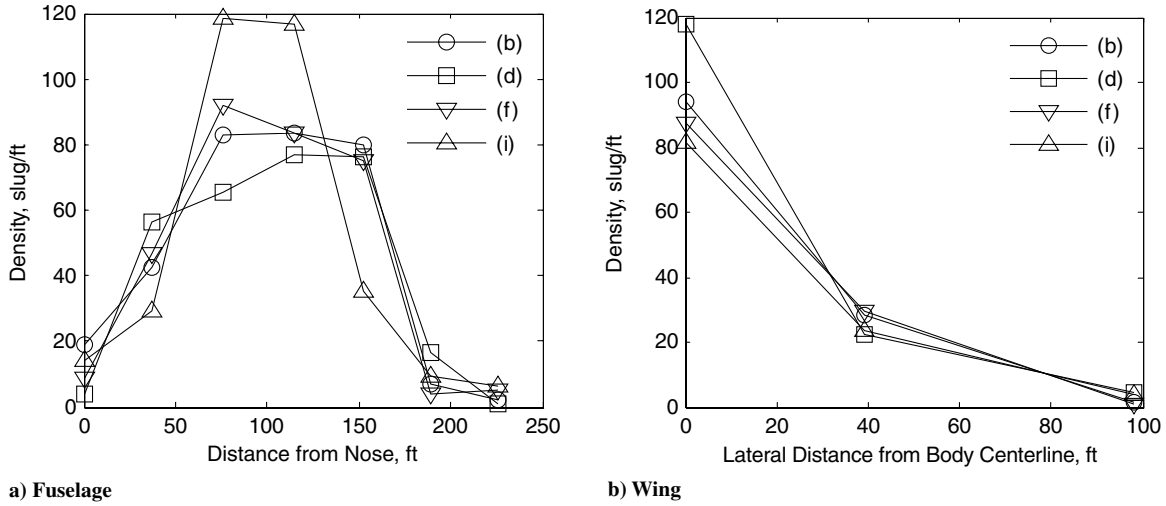

a) Fuselage **b) Wing**

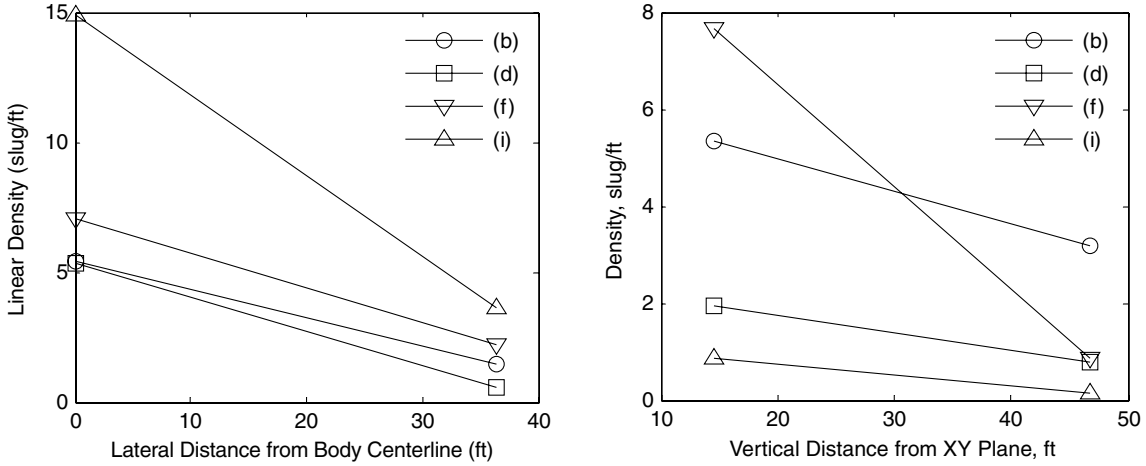

c) Horizontal tail **d) Vertical tail**

Fig. 13 Mass density variations of selected tailored solutions [cases (b), (d), (f), and (i) from Fig. 12].

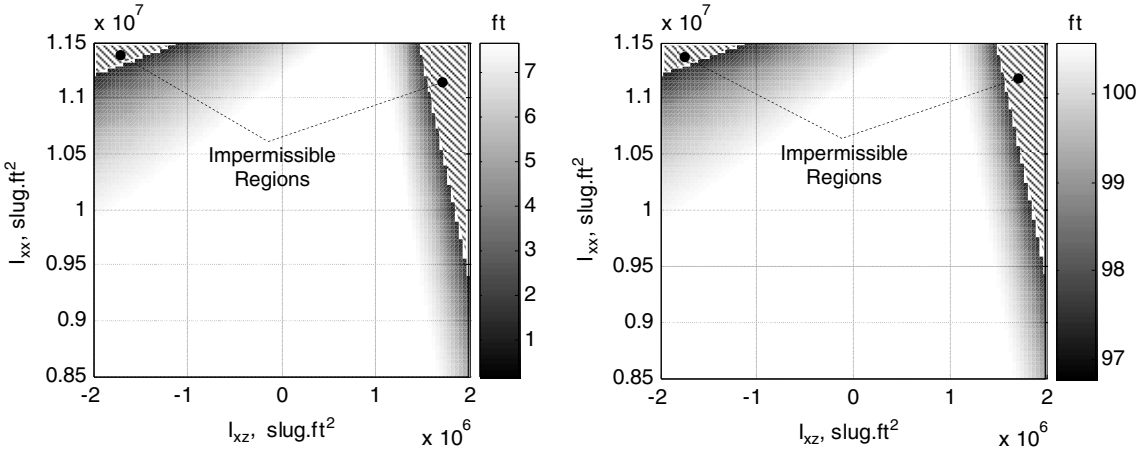

Fig. 14 Allowable c.g. travel (left) and mean longitudinal c.g. positions (right) in cruising flight (ft).

freedom reduces as constraints increase. This feature offers a powerful tool to manage inertia terms in a systematic manner during aircraft preliminary and in some cases in detailed design.

V. Conclusions and Discussion

The MDM technique is a promising tool that helps take into account flying qualities via inertia terms and mass distribution of an aircraft in early stages of the design process. Together with an efficient optimization algorithm such as GSS, the design team would be able to study not just external but different internal arrangements as design progresses. The case studies of this work describe a method to find a set of optimal mass distribution patterns for a given external shape in two flight conditions; nevertheless, different case studies conducted by the authors show that the number of flight conditions could easily be increased [4]. However, for flight conditions equal to four and more, it would be extremely difficult to find a mass

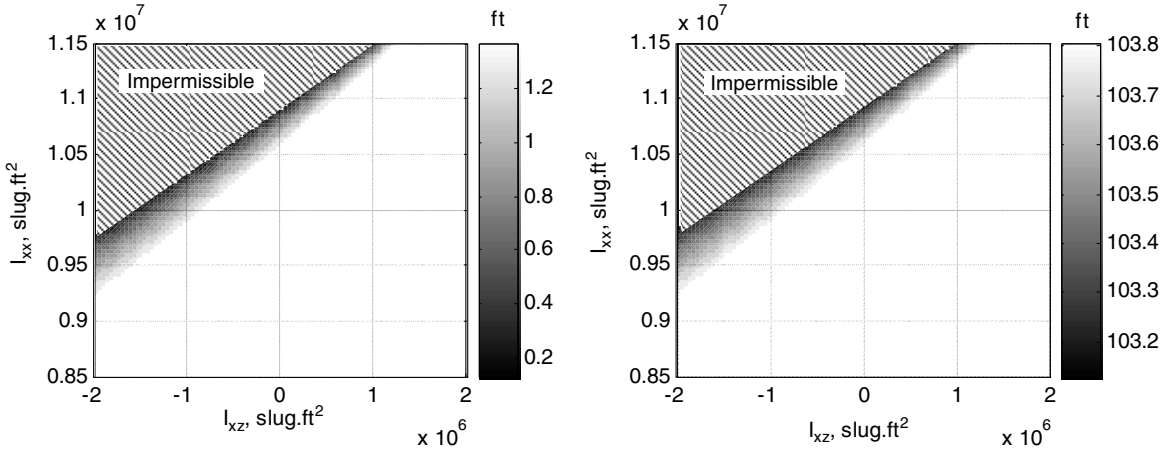

Fig. 15 Allowable c.g. travel (left) and mean longitudinal c.g. positions (right) in turning flight (ft).

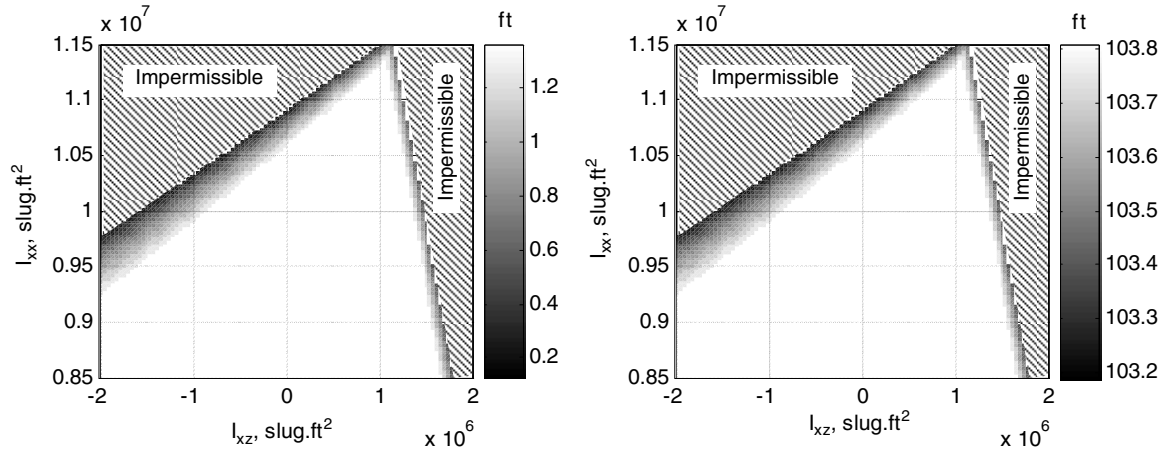

Fig. 16 Allowable c.g. travel (left) and mean longitudinal c.g. positions (right) in cruising and turning flights (ft).

distribution, which optimizes all FQ to the level-I requirements. In such cases, designers might expect some level-II requirements or might think of using the stability augmentation system (SAS) or MEGCS as introduced earlier in the paper. We, the authors, do not wish to go into further detail of how a MEGCS might work. In fact, the idea of developing a MEGCS is an outcome of this work. The concept of MEGCS seems to be attractive; nevertheless further investigation is necessary as to how it might be designed.

Another important outcome of MDM is a systematic approach to evaluate whether all mission phases of an aircraft are consistent or not. That is, considering all flight conditions, if MDM leads to any mass distribution where all modes meet level-I requirements. Then we might conclude that all mission phases are in fact consistent and the aircraft is not penalized in some phases of its mission. On the contrary, if no mass distribution is found, then one might conclude that mission phases are not consistent or what we expect from aircraft to perform in different flight phases is not consistent with one another. As an example, we might consider an aircraft with very long range or endurance while having a low cruising altitude. In such cases, we might think of changing the aircraft's external shape to suit the mission. The other possibility is of course to use MDM as a tool to change the mission to a more consistent one where MDM provides some solutions. Generalization of the MDM concept to include a complete flight envelope is therefore a very attractive way to evaluate a mission profile in early stages of the design. The technique would also help to find those flight phases where designers need to think of devices to change the external shape of the aircraft. In fact, concepts such as "fuel management" and "mission adaptive wings" [6] could very well be predicted and justified by the MDM technique. Even if a design team might not accept some of the mass distribution patterns, MDM can still bring more insight to design a better aircraft.

References

[1] Malaek, S. M., and Soltan-Mohammed, B., "Mass Distribution Management and Dynamic Balancing of Aircraft Mass," *Aircraft Design Journal*, Vol. 4, No. 1, March 2001, pp. 51–61. doi:10.1016/S1369-8869(00)00024-0

[2] Anon., "Military Specifications–Flying Qualities of Piloted Airplanes," MIL F-8785C, 1987.

[3] Roskam J., *Airplane Flight Dynamics and Automatic Flight Control*, DARCORP, Lawrence, KS, 1990.

[4] Karimi, A., "Development of Mathematical Tools to Support MDM," M.S. Thesis, Aerospace Engineering Department, Sharif University of Technology, Tehran, Iran, 2006 (available in Persian).

[5] Hodgkinson, J., *Aircraft Handling Qualities*, Blackwell Science, London, 1998.

[6] Roskam J., *Airplane Design Series*, DARCORP, Lawrence, KS, 1991, Pts. I–8.

[7] Chelouah, R., and Siarry, P., "A Continuous Genetic Algorithm Designed for the Global Optimization of Multimodal Functions," *Journal of Heuristics*, Vol. 6, No. 2, June 2000, pp. 191–213. doi:10.1023/A:1009626110229

[8] Chelouah, R., and Siarry, P., "Genetic and Nelder–Mead Algorithms Hybridized for a More Accurate Global Optimization of Continuous Multiminima Functions," *European Journal of Operational Research*, Vol. 148, No. 2, July 2003, pp. 335–348. doi:10.1016/S0377-2217(02)00401-0

[9] Nelder, J. A., and Mead, R., "A Simplex Method for Function Minimization," *Computer Journal*, Vol. 7, 1965, pp. 308–313.

[10] Tsutsi, S., Yamamura, M., and Higuchi, T., "Multi-Parent Recombination with Simplex Crossover in Real Coded Genetic

Algorithmsm," *Proceedings of the GECCO-99*, Morgan Kaufmann, Orlando, FL, 1999, pp. 657–664.

[11] Higuchi, T., Tsutsui, S., and Yamamura, M., "Theoretical Analysis of Simplex Crossover for Real-Coded Genetic Algorithms," *Proceedings of the PPSN VI*, Springer–Verlag, Paris, 2000, pp. 365–374.

[12] Hedar, A., and Fukushima, M., "Minimizing Multimodal Functions by Simplex Coding Genetic Algorithm," *Optimization Methods and Software*, Vol. 18, No. 3, 2003, pp. 265–282.

[13] Renders, J. M. and Bersini, H., "Hybridizing Genetic Algorithms with Hill-Climbing Methods for Global Optimization: Two Possible Ways," *Proceedings of the First IEEE Conference on Evolutionary Computation*, edited by Z. Michalewicz, J. D. Schaffer, H. P. Schwefel, D. B. Fogel, and H. Kitano, IEEE, Piscataway, NJ, 1994, pp. 312–317.

[14] Yen, J., Liao, J. C., Bogju, L., and Randolph, D., "A Hybrid Approach to Modeling Metabolic Systems Using a Genetic Algorithm and Simplex Method," *IEEE Transactions on Systems, Man, and Cybernetics*, Vol. 28, No. 2, 1998, pp. 173–191. doi:10.1109/3477.662758

[15] Sotiropoulos, D. G., Plagianakos, V. P., and Vrahatis, M. N., "An Evolutionary Algorithm for Minimizing Multimodal Functions," *Proceedings of the Fifth Hellenic-European Conference on Computer Mathematics and its Applications (HERCMA 2001)*, edited by E. A. Lipitakis, Vol. 2, LEA Press, Athens, 2002, pp. 496–500.